FIFTH INTERNATIONAL CONGRESS ON SOUND AND VIBRATION
DECEMBER 15-18, 1997
ADELAIDE, SOUTH AUSTRALIA

Acoustic and Elastic Wave Scattering from A Rigid or Soft Cylinder

Huinam Rhee
Reactor Mechanical Engineering,
Korea Power Engineering Company, Taejon 305-353, Korea

Youngjin Park
NOViC, Department of Mechanical Engineering,
Korea Advanced Institute of Science and Technology, Taejon, 305-701, Korea

ABSTRACT

Classical acoustic and elastic wave scattering problems from an acoustically rigid or soft cylinder are revisited. The behavior of *phases* as well as magnitudes of each partial waves and form functions are numerically analyzed and discussed. The effect of *mode conversion*, especially, on the *phases* of each partial waves in elastic wave scattering is identified.

INTRODUCTION

Recently, the behavior of phases of resonances isolated from partial waves for acoustic wave resonance scattering were analyzed by a novel acoustic wave resonance scattering formalism using the concept of the *resonance scattering function* by Rhee and Park[1]. By using this new formalism, the phases of resonances of an *elastic* or *fluid* target, which are isolated by the proper *background*, are shifted by π radians through each resonances and anti-resonances. These π -phase shifts have not been explicitly obtained by previous works[2-9]. However, for elastic wave scattering problems[10], the isolated resonances show different behaviors of phases, that is, exact π -phase shifts are not generally obtained due to *mode conversion*. In order to identify the effect of *mode conversion* more clearly, this paper deals with acoustic and elastic wave scatterings from impenetrable bodies as simple examples. Previous studies on this subject usually discussed only scattering magnitudes except some limited discussions on phases.[2,3] After briefly reviewing the theory of scattering, we will proceed to the main discussion on the behaviors of *phases* and magnitudes of scattered waves for acoustic and elastic wave scatterings from an infinitely-long impenetrable cylinder.

1. ACOUSTIC WAVE SCATTERING[2]

Let us consider an infinite plane acoustic wave $p_0 \exp i(kx - \omega t)$ with a propagation constant $k = \omega / c$, incident along the x - axis on a rigid or soft cylinder of radius a whose axis is coincides with the z - axis. The acoustic impedance of the rigid (soft) cylinder is infinite (zero) so that the incident wave can not penetrate into the cylinder at all. At a point $P(r,\phi)$ located in the fluid surrounding the cylinder, it produces the following scattered field P_{sc}:

$$P_{sc}(r,\phi) = p_0 \sum_{n=0}^{\infty} \varepsilon_n i^n A_n(x) H_n^{(1)}(kr) \cos n\phi, \tag{1}$$

By applying appropriate boundary conditions, the coefficient A_n is determined as follows:

$$A_n(x) = A_n(x)^r = -\frac{J_n'(x)}{H_n^{(1)'}(x)} \qquad \text{(for a rigid cylinder)}, \tag{2}$$

$$A_n(x) = A_n(x)^s = -\frac{J_n(x)}{H_n^{(1)}(x)} \qquad \text{(for a soft cylinder)}, \tag{3}$$

where p_0 is the incident pressure amplitude, ε_n is the Neumann factor ($\varepsilon_n = 2\text{-}\delta_{n0}$), J_n and $H_n^{(1)}$ are the Bessel function and the Hankel function of the first kind, respectively. The argument x of the cylindrical functions is $x = ka = \omega a / c_w$, where c_w is the speed of sound in the fluid. The prime denotes differentiation with respect to the argument. By using the asymptotic form of Hankel function, the farfield scattered pressure becomes

$$P_{sc}(\phi) = p_0 e^{ikr} \sqrt{\frac{2}{\pi i k r}} \sum_{n=0}^{\infty} \varepsilon_n i^n A_n(x) \cos n\phi, \quad r >> a. \tag{4}$$

The form function f_∞ is defined as a summation of normal modes or partial waves:

$$f_\infty(\phi) = \sqrt{\frac{r}{a}} \frac{P_{sc}}{p_0} e^{-ikr} = \sum_{n=0}^{\infty} f_n(\phi) = \sqrt{\frac{2}{\pi i x}} \sum_{n=0}^{\infty} \varepsilon_n A_n(x) \cos n\phi. \tag{5}$$

2. ELASTIC WAVE SCATTERING[5]

2.1 *P*-wave incidence case

A plane *P* wave incident along the *x* axis can be expressed as a partial wave series,

$$\varphi_{inc} = \varphi_0 \exp i(k_p x - \omega t) = \varphi_0 \sum_{n=0}^{\infty} \varepsilon_n i^n J_n(k_p r) \cos n\phi, \tag{6}$$

where $k_p = \omega / c_p$ is the longitudinal wave number. It produces scattered elastic waves which have the following form of potentials:

$$\varphi_{sc} = \sum_{n=0}^{\infty} \varepsilon_n i^n A_n H_n^{(1)}(k_p r) \cos n\phi, \tag{7}$$

$$\psi_{sc} = \sum_{n=0}^{\infty} \varepsilon_n i^n B_n H_n^{(1)}(k_s r) \sin n\phi, \tag{8}$$

where $k_s = \omega / c_s$ is the transversal wave number.

Eqs.(9) and (10) represent outgoing *P* and *S* waves with wave number k_p and k_s, respectively. In eq.(10) the incident *P* wave generated an outgoing *S* wave, which represents a phenomenon known as *mode conversion*. By applying a set of appropriate boundary

conditions, the coefficients A_n and B_n are determined as:

For a rigid cylinder,

$$A_n^r = \begin{vmatrix} -\mathrm{Re}\,a_{11} & a_{12} \\ -\mathrm{Re}\,a_{21} & a_{22} \end{vmatrix} \Big/ \begin{vmatrix} a_{11} & a_{12} \\ a_{21} & a_{22} \end{vmatrix}, \qquad B_n^r = \begin{vmatrix} a_{11} & -\mathrm{Re}\,a_{12} \\ a_{21} & -\mathrm{Re}\,a_{22} \end{vmatrix} \Big/ \begin{vmatrix} a_{11} & a_{12} \\ a_{21} & a_{22} \end{vmatrix}, \tag{9}$$

where $a_{11} = x_p H_n^{(1)'}(x_p)$, $a_{12} = nH_n^{(1)}(x_s)$, $a_{21} = -nH_n^{(1)'}(x_p)$, $a_{22} = -x_s H_n^{(1)'}(x_s)$, $x_{p,s} = k_{p,s}a$ and the superscript r denotes *rigid*.

For a soft cylinder,

$$A_n^s = \begin{vmatrix} -\mathrm{Re}\,b_{11} & b_{12} \\ -\mathrm{Re}\,b_{21} & b_{22} \end{vmatrix} \Big/ \begin{vmatrix} b_{11} & b_{12} \\ b_{21} & b_{22} \end{vmatrix}, \qquad B_n^s = \begin{vmatrix} b_{11} & -\mathrm{Re}\,b_{11} \\ b_{21} & -\mathrm{Re}\,b_{21} \end{vmatrix} \Big/ \begin{vmatrix} b_{11} & b_{12} \\ b_{21} & b_{22} \end{vmatrix}, \tag{10}$$

where

$b_{11} = -x_s^{\,2} H_n^{(1)}(x_p) - 2x_p H_n^{(1)'}(x_p) + 2n^2 H_n^{(1)}(x_p)$, $b_{12} = -2nH_n^{(1)}(x_s) + 2nx_s H_n^{(1)'}(x_s)$,

$b_{21} = 2nH_n^{(1)}(x_p) - 2nx_p H_n^{(1)'}(x_p)$, $b_{22} = x_s^{\,2} H_n^{(1)}(x_s) + 2x_s H_n^{(1)'}(x_s) - 2n^2 H_n^{(1)'}(x_s)$, and the superscript s denotes *soft*.

The far field *form function* f_∞ is defined as a summation of normal modes:

$$f_\infty^{pp}(\phi) = \sum_{n=0}^{\infty} f_n^{pp}(\phi) = \sqrt{\frac{2}{\pi i x_p}} \sum_{n=0}^{\infty} \varepsilon_n A_n \cos n\phi\,, \tag{11}$$

$$f_\infty^{ps}(\phi) = \sum_{n=0}^{\infty} f_n^{ps}(\phi) = \sqrt{\frac{2}{\pi i x_s}} \sum_{n=0}^{\infty} \varepsilon_n B_n \sin n\phi\,. \tag{12}$$

2.2 *S* wave incidence case

A plane *S* wave incident along the x axis can be expressed as a partial wave series,

$$\psi_{inc} = \psi_0 \exp i(k_s x - \omega t) = \psi_0 \sum_{n=0}^{\infty} \varepsilon_n i^n J_n(k_s r) \cos n\phi\,, \tag{13}$$

It produces scattered elastic waves which have the following form of potentials:

$$\varphi_{sc} = \sum_{n=0}^{\infty} \varepsilon_n i^n C_n H_n^{(1)}(k_p r) \sin n\phi\,, \tag{14}$$

$$\psi_{sc} = \sum_{n=0}^{\infty} \varepsilon_n i^n D_n H_n^{(1)}(k_s r) \cos n\phi\,. \tag{15}$$

By applying a set of boundary conditions, the coefficients C_n and D_n are determined as:

$$C_n^r = \begin{vmatrix} -\mathrm{Re}\,c_{12} & c_{12} \\ -\mathrm{Re}\,c_{22} & c_{22} \end{vmatrix} \Big/ \begin{vmatrix} c_{11} & c_{12} \\ c_{21} & c_{22} \end{vmatrix}, \qquad D_n^r = \begin{vmatrix} c_{11} & -\mathrm{Re}\,c_{12} \\ c_{21} & -\mathrm{Re}\,c_{22} \end{vmatrix} \Big/ \begin{vmatrix} c_{11} & c_{12} \\ c_{21} & c_{22} \end{vmatrix}, \tag{16}$$

where $c_{11} = a_{11}$, $c_{12} = -a_{12}$, $c_{21} = -a_{21}$, $c_{22} = a_{22}$, and a_{ij} is defined in Eq.(9).

$$C_n^s = \begin{vmatrix} -\mathrm{Re}\,d_{12} & d_{12} \\ -\mathrm{Re}\,d_{22} & d_{22} \end{vmatrix} \Big/ \begin{vmatrix} d_{11} & d_{12} \\ d_{21} & d_{22} \end{vmatrix}, \qquad D_n^s = \begin{vmatrix} d_{11} & -\mathrm{Re}\,d_{12} \\ d_{21} & -\mathrm{Re}\,d_{22} \end{vmatrix} \Big/ \begin{vmatrix} d_{11} & d_{12} \\ d_{21} & d_{22} \end{vmatrix}, \tag{17}$$

where $d_{11} = b_{11}$, $d_{12} = -b_{12}$, $d_{21} = -b_{21}$, $d_{22} = b_{22}$, and b_{ij} is defined in Eq.(10).

The far field *form function* f_∞ is defined as a summation of normal modes:

$$f_{\infty}^{sp}(\phi) = \sum_{n=0}^{\infty} f_n^{sp}(\phi) = \sqrt{\frac{2}{\pi i x_p}} \sum_{n=0}^{\infty} \varepsilon_n C_n \sin n\phi \,, \tag{18}$$

$$f_{\infty}^{ss}(\phi) = \sum_{n=0}^{\infty} f_n^{ss}(\phi) = \sqrt{\frac{2}{\pi i x_s}} \sum_{n=0}^{\infty} \varepsilon_n D_n \cos n\phi \,. \tag{19}$$

3. NUMERICAL ANALYSIS AND DISCUSSION

For numerical calculations, the *fluid* or *elastic* medium is assumed to be water or aluminum, respectively. The longitudinal wave speed of water is 1480 m/sec, and the longitudinal and transversal wave speeds of aluminum are 6370 and 3070 m/sec, respectively. All numerical calculations are performed for backscattering, that is, $\phi = \pi$.

3-1 Rigid cylinder

Fig. 1 compares magnitudes and phases of partial waves of the elastic rigid *PP* case with the acoustic rigid case. These two cases are comparable because we have only *PP* case for the acoustic wave scattering. For n=0 mode, *mode conversion* does not occur for the elastic wave scattering. In Fig. 1(a) we obtain identical magnitude and phase for both cases. We note that the dips in the magnitude between two neighboring smooth peaks reaches to zero and abrupt π -phase shifts occur at dip frequencies. The amount of phase shifts through the peaks are also π . For $n \geq 1$, while acoustic wave scattering keeps this behavior, elastic wave scattering does not. As an example, for n=3, Fig. 1(b) and (c) show that the magnitudes never reach to the zero even at the dips, and the phase shifts at the dips as well as through the smooth peaks are less than π radians. (Gaunaurd *et al.*[3,4] mentioned this *non-zero(filled- in) dip* was due to *mode conversion* and *radiation damping*. However, we can see that *radiation damping* is not contributing to this *filled-in dip* because acoustic scattering does not show any *filled-in dip*.) These phenomena are more apparent in the low frequency region as shown in Fig. 1(b). As the frequency becomes higher, at the dip frequencies the magnitudes approach to zero and the phase shifts become close to π . Fig. 1(c) shows clearly that the phase shift at a dip for elastic wave scattering is not abrupt but *gradual*. These phenomena are due to *mode conversion*. The energy of incidence *P* wave is partially converted to that of *S* wave during elastic wave scattering when $n \geq 1$. By introducing the analogy of mechanical vibration system, *PP* case acts like a system with damped oscillators, in which the phase shift at a resonance is gradual and less than π due to the energy dissipation by damping and the overlapping of neighboring resonances. The amount of mode converted energy is larger in the low frequency region and becomes smaller as the frequency increases, as shown in *PS* case in Fig. 1(d). The elastic *PS* case looks much simpler than *PP* case : There is only one smooth peak in the magnitude which moves to the right as the mode number n increases, and therefore no dip exists. The phase goes down smoothly without any abrupt shift as the frequency increases.

Due to the unitarity of the scattering matrix, the *PS* and *SP* cases are identical (except the different level of magnitude). Fig. 2 presents the *SS* case. Similarly to the *P*-wave incidence case, there is no mode conversion when $n = 0$. Fig. 2(a) shows that for $n = 0$ mode, dips reaches to zero in magnitude and π -phase shifts take place at the dip frequencies and also through smooth peaks. (We note that if Fig. 2(a) is plotted as a function of $k_s a$ rather than

$k_p a$, it would be the identical plot as Fig. 1(a).) Like the *PP* case, for $n \geq 1$, the dips do not reach down to zero and the phase shifts are less than π radians because of *mode conversion,* as shown in Fig. 2(b).

The form functions can simply be obtained by summing partial waves by the definition. We will not show the plots in this paper. However, we want to note that the magnitudes of the form functions for non-mode conversion cases (*PP* or *SS*) converges to the same value of $1/\sqrt{2}$ for both acoustic and elastic wave scatterings, and the phases are smoothly decreasing without any abrupt (or gradual) phase shift although each partial waves include phase shifts at the dip frequencies.

3-2 Soft cylinder

Basically, the same trends in the behaviors of magnitudes and phases were found for both the rigid and soft cylinder cases. Therefore, the detailed discussion is not repeated for the soft cylinder case.

Elastic *soft PP* n=0 mode in Fig. 3(a) behaves differently from acoustic *soft* n=0 mode, especially, near zero frequency, while we had identical plots for *elastic rigid PP* and *acoustic rigid* for n=0 mode (Fig. 1(a)). A parametric study was performed in Fig. 4, where the shear wave velocity c_s of the elastic medium is arbitrarily decreased from 3070 m/s to 0.1 m/s to simulate acoustic wave scattering. As c_s decreases, a larger peak is clearly shown of which location is approaching to the zero frequency. For c_s=0.1 m/s, it shows almost same magnitude and phase with the acoustic n=0 mode (Fig. 4(a)). However, more detailed calculation shows that there is still a very high peak near zero frequency as can be seen in Fig. 4(b). This peak was mentioned as a *giant monopole* elsewhere[5]. Therefore, we can see that the *giant monopole* is caused by diminishing shear wave velocity c_s due to the loss of shear resistance in the medium. *PS* case shown in Fig. 5 presents two smooth peaks (of which locations are moving to the high frequency region and of which magnitudes decrease as the mode number increases). The phase smoothly goes down through the second peak without any shift. A dip existing between these two peaks reaches to zero in magnitude and the abrupt phase shift of π occurs at the dip frequency. This dip moves to the right as the mode number n increases. This behavior of elastic soft *PS* case looks different from *PP* case ($n \geq 1$) and can be explained as such: There is an energy loss in *PP* case, and consequently *PS* case earns the energy which *PP* loses. Therefore, elastic soft *PS* case is not comparable to a damped oscillator, but rather a negatively damped one. Fig. 5 also shows that the dip exists at the exactly same frequency for both *PS* and *SP* cases. As shown in Fig. 6, we observed that for *SS* cases when $n \geq 2$, the first dip from the left side is very close to zero magnitude and the phase shift is close to π radians at that frequency. This is because the mode converted energy is very small near this first dip frequency as can be seen in Fig. 5.

The form functions can be obtained by summing partial waves. Fig. 7 shows the form function of elastic soft *SS* case, which appeared to be the most noteworthy shape. It is due to the characteristics of interference between two shear waves from the reflection on and diffraction around the soft cylinder.

4. CONCLUSIONS

The different phenomena between the acoustic and elastic wave scatterings were

discussed. In case of non-mode conversion in the acoustic or elastic wave scattering, the dip between smooth peaks of each partial wave reaches down to the zero magnitude and the *abrupt* π - *phase shift* occurs at the dip frequency. However, for *mode conversion* cases the dip never reaches to zero magnitude, and the phase shift becomes *gradual* and *less than* π. The phases of the form functions do not show any phase shift throughout all the frequencies.

[1]Huinam Rhee and Youngjin Park, "Novel acoustic wave resonance scattering formalism", J. Acoust. Soc. Am., accepted for publication.

[2]L.Flax, L. R. Dragonette, and H. Uberall, "Theory of elastic resonance excitation by sound scattering", J. Acoust. Soc. Am. **63**(3), 723-731 (1978).

[3]G.C.Gaunaurd, H. Uberall, "Theory of resonance scattering from spherical cavities in elastic and viscoelastic media," J. Acous. Soc. Am., **63**(6), 1699-1712 (1978).

[4]G.C.Gaunaurd, H. Uberall, "Numerical evaluation of modal resonances in the echoes of compressional waves scattered from fluid-filled spherical cavities in solids," J. Appl. Phys. **50**(7), 4642-4660 (1979).

[5]L. Flax, G. Gaunaurd, and H. Uberall, "Theory of Resonance Scattering", in *Physical Acoustics*, edited by W. P. Mason and R. N. Thurston (Acamedic, New York, 1981), Vol.XV, pp191-294.

[6]H. Uberall, "Acoustic Resonance Scattering", Gordon and Breach Science Publishers, 1992.

[7]N. D. Veksler, "Resonance Acoustic Spectroscopy", Springer-Verlag, 1993.

[8]G. C. Gaunaurd, "Elastic and acoustic resonance wave scattering", Appl . Mech . Rev. **42**(6), June 1989.

[9]G. C. Gaunaurd, M. F. Werby, "Acoustic resonance scattering by submerged elastic shells", Appl . Mech . Rev. **43**(8), August 1990.

[10]Huinam Rhee and Youngjin Park, "Novel elastic wave resonance scattering formalism", submitted to J. Acoust. Soc. Am.

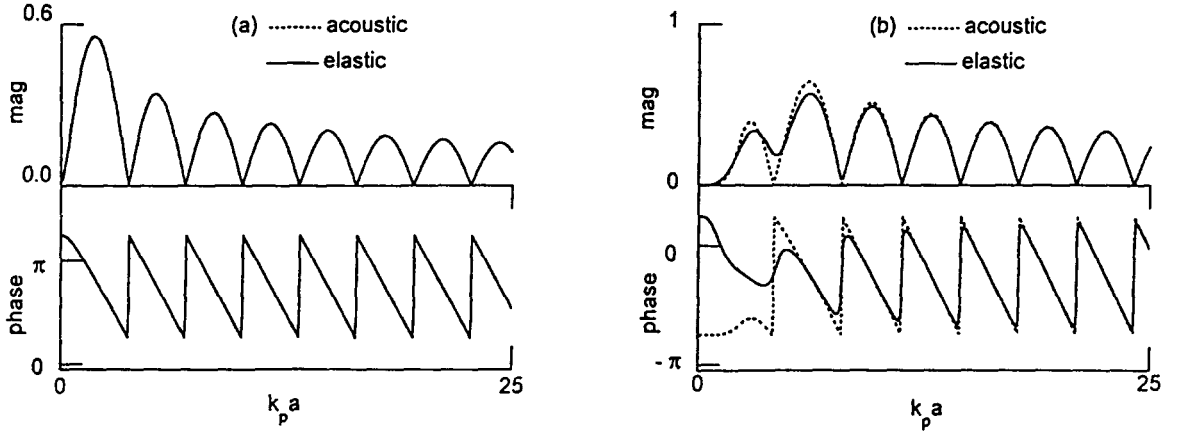

FIG. 1 Acoustic and elastic wave scattering (*P* wave incidence) from a rigid cylinder: (a)*PP* n=0 (b)*PP* n=3 (c)*PP* n=3 zoomed plot and (d) *PS*.

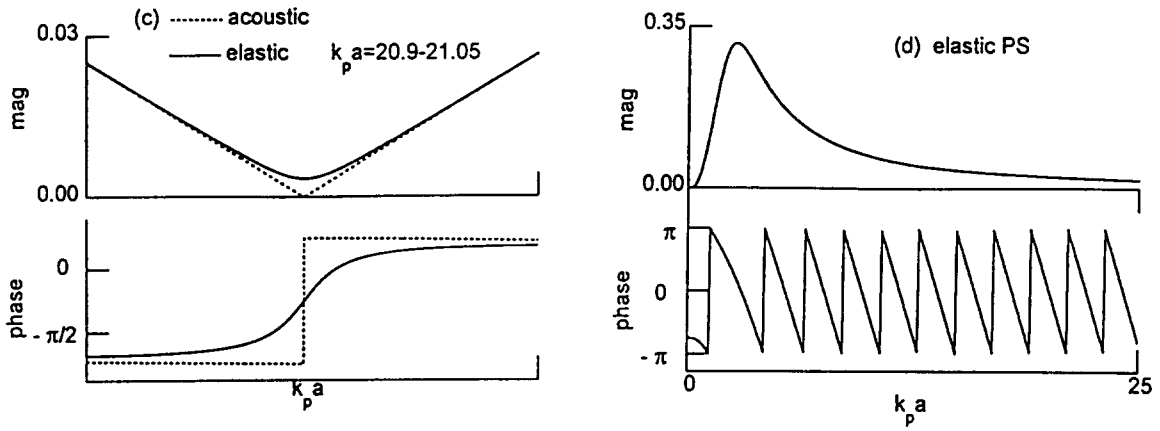

FIG. 1 (Continued)

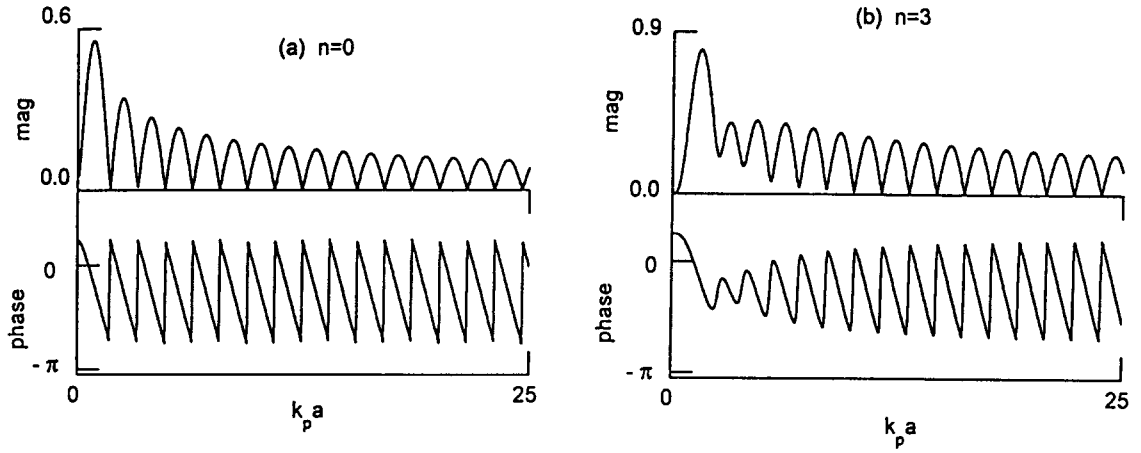

FIG. 2 Elastic wave scattering (*SS*) from a rigid cylinder: (a) n=0 and (b) n=3.

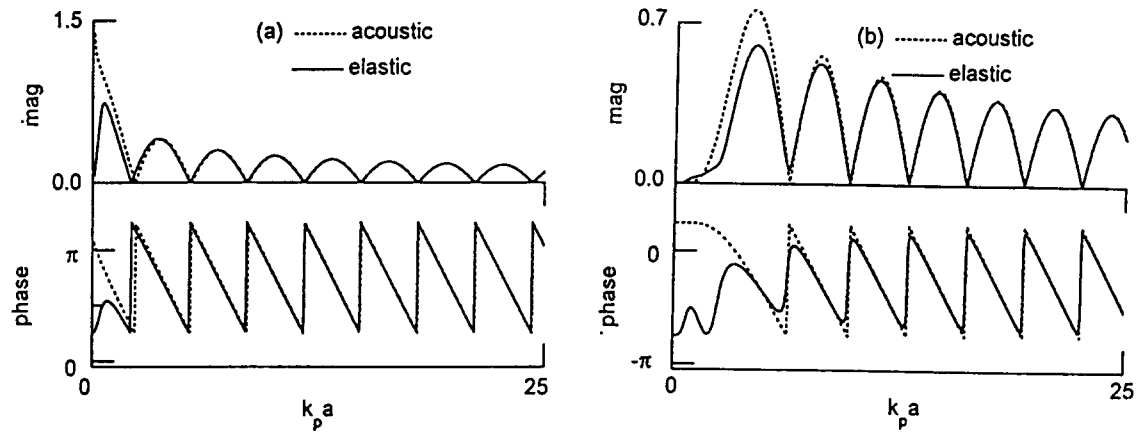

FIG. 3 Acoustic and elastic wave scattering (*PP*) from a soft cylinder: (a) n=0 and (b) n=3.

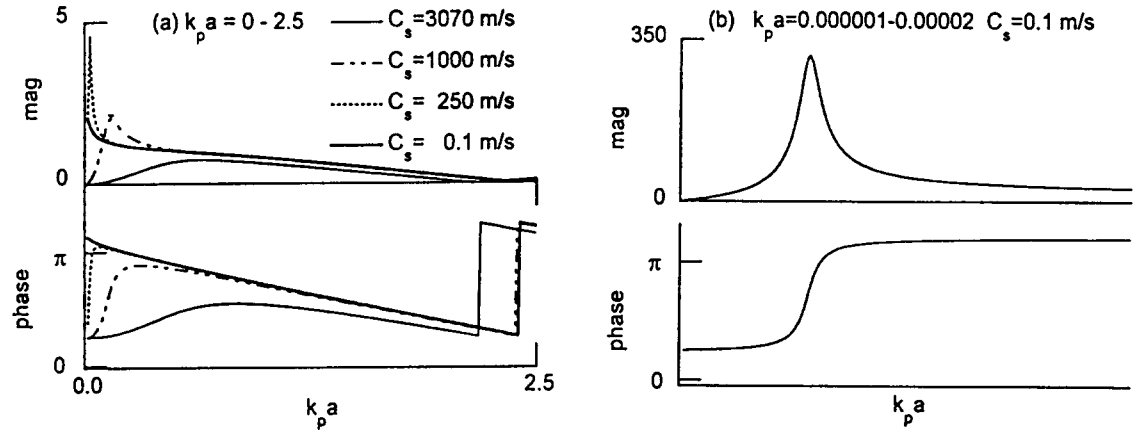

FIG. 4 Elastic wave scattering (*PP*) from a soft cylinder with a varying c_s: (a) n=0, $k_p a$ = 0 - 2.5 and (b) n=0, $k_p a$ = 0.000001 - 0.00002.

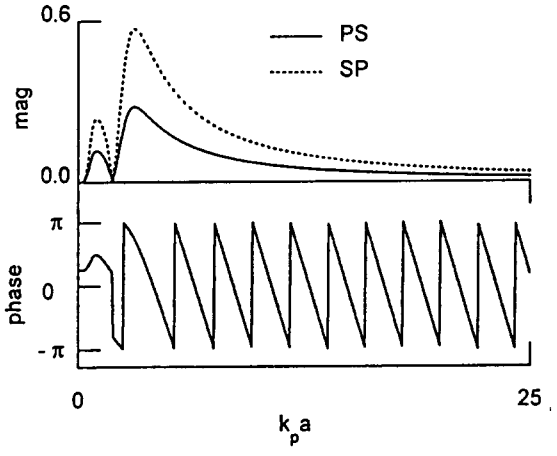

FIG. 5 Elastic wave scattering (*PS* and *SP*) from a soft cylinder for n=3.

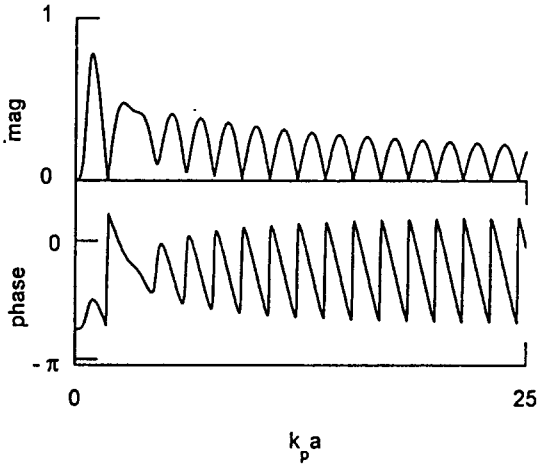

FIG. 6 Elastic wave scattering (*SS*) from a soft cylinder for n=3.

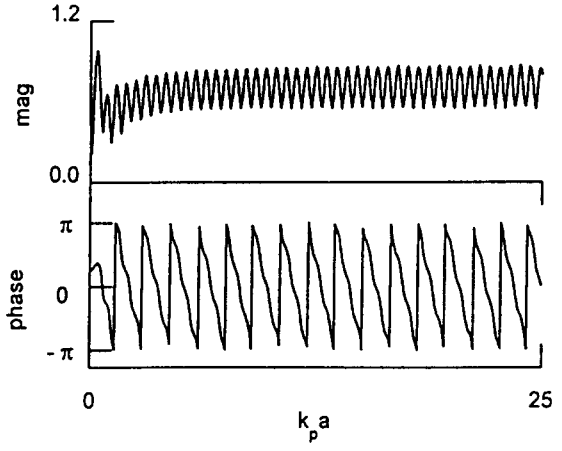

FIG. 7 Form function for elastic wave scattering (*SS*) from a soft cylinder.